



DE95707386

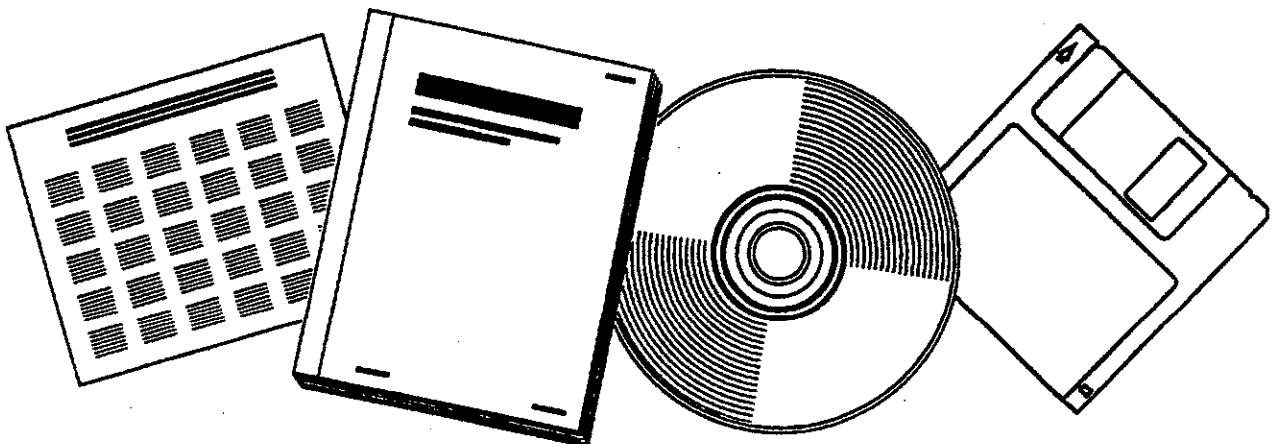
**NTIS**<sup>®</sup>  
Information is our business.

---

# CO HYDROGENATION OVER COBALT FISCHER-TROPSCH CATALYSTS

NORGES TEKNISKE HOEGSKOLE, TRONDHEIM

OCT 1993



U.S. DEPARTMENT OF COMMERCE  
National Technical Information Service

---

A Thesis Submitted

to

*The Department of Industrial Chemistry*

*The Norwegian Institute of Technology*

*The University of Trondheim*

In Partial Fulfillment of the Requirements

of the Degree

DOCTOR OF ENGINEERING

October 1993

**MASTER**

## ABSTRACT

The main aim of the present work has been to study in what way the addition of a second metal influences the CO hydrogenation rate over alumina supported cobalt catalysts.

Temperature programmed reduction studies (298 - 1173 K) show that calcined 9%Co/Al<sub>2</sub>O<sub>3</sub> contains two main cobalt phases: Crystalline Co<sub>3</sub>O<sub>4</sub> particles and a cobalt oxide layer containing cobalt ions interacting with the alumina support surface. Some amounts of heavily reducible CoAl<sub>2</sub>O<sub>4</sub> are also present in the catalyst. Addition of 0.1 and 1.0 wt% Pt from a chloride containing precursor lowers the temperature for Co<sub>3</sub>O<sub>4</sub> reduction with about 80 K, while the reduction temperature of the oxidic cobalt surface layer is lowered with 100 - 200 K compared to the monometallic cobalt catalyst. The temperature shift increases with increasing platinum amount. 1 wt% Pt from a chloride free platinum precursor increases the shift for the reduction of Co<sub>3</sub>O<sub>4</sub> to 140 K, while reduction of the cobalt surface phase is shifted 100 K compared to the monometallic catalyst.

Other second metals (Pd, Ru, Ir or Re) also lowers the cobalt reduction temperature. The size of the shift depends on the type of metal. It is suggested that the second metal must be reduced itself before it promotes the reduction of cobalt.

It is found that the bimetallic CoPt and CoRe catalysts are reduced to a larger extent compared to the monometallic cobalt catalyst during an isothermal reduction for 16 hours at 623 K. In the bimetallic catalysts the oxidic cobalt surface layer are reduced, while this is not the case for the monometallic catalyst.

Both the extent of decomposition of cobalt nitrate during the calcination and the reductive decomposition temperature are unaffected by addition of a second metal.

Temperature programmed reduction also shows that increasing the calcination temperature from 573 to 698 K increases the extent of oxydative decomposition of cobalt nitrate, and lowers the amount of oxidic cobalt surface layer. The amount of cobalt as Co<sub>3</sub>O<sub>4</sub> particles remains constant with increasing calcination temperature in this range. It is assumed that Co<sup>2+</sup>

diffusion from the surface layer into the alumina lattice increases with increasing calcination temperature, giving more heavily reducible  $\text{CoAl}_2\text{O}_4$ .

Volumetric chemisorption measurements at 298 K show that both Pt and Re addition to 9%Co/ $\text{Al}_2\text{O}_3$  results in a large increase in CO adsorption. The  $\text{H}_2$  adsorption increases also with addition of Pt and Re, but the increase is smaller for Re addition compared to Pt addition. The difference between the two promoted catalysts is assumed to be due to hydrogen adsorption on Pt. Both CO and  $\text{H}_2$  adsorption increases with increasing amount of Pt addition.

The CO:H adsorption ratio increases in the order



Chemisorption of  $\text{H}_2$  on chloride containing, platinum promoted catalysts shows that these catalysts adsorb somewhat less hydrogen compared with the monometallic cobalt catalyst. Increased calcination temperature of the 9%Co/ $\text{Al}_2\text{O}_3$  catalyst also slightly decreases the  $\text{H}_2$  uptake on the catalyst.

Activity measurements done with differential conditions at 473 K and 1 bara show that promotion of the cobalt catalyst with Pt or Re increases the rate of CO conversion to hydrocarbons. Re addition gives the largest increase. The increase in CO conversion over the rhenium promoted catalyst is larger than the increase in  $\text{H}_2$  uptake. The increase in CO conversion rate over the platinum promoted catalyst is in agreement with the observed increase in degree of reduction and the increase in  $\text{H}_2$  uptake. However, some of the hydrogen uptake was considered to be on platinum. Promotion with rhenium as well as platinum then gives increased turnover frequency on the cobalt sites. The results therefore indicate that the increase in rate for both the Pt and the Re promoted catalysts is due to increased number of active sites, and also probably to increased intrinsic activity.

Activity measurements done with differential conditions at 513 K and 7 bara did not show any differences between the unpromoted and the promoted catalysts. It is suggested that the reaction rates in this case are limited by the reactant diffusion through liquid products present in the catalyst pores.

Selectivity measurements did not show significant differences in hydrocarbon chain length between the unpromoted and platinum promoted cobalt catalysts, but a decreased  $\alpha$ -olefin/n-paraffin ratio could be observed with increasing platinum addition.

## CONTENTS

### ABSTRACT

### ACKNOWLEDGEMENTS

### LIST OF SYMBOLS AND ABBREVIATIONS

### LIST OF FIGURES AND TABLES

1 INTRODUCTION .....	1
1.1 The Fischer-Tropsch synthesis history .....	1
1.2 Fischer-Tropsch synthesis today .....	2
1.3 Objectives of the present work .....	4
1.4 SPUNG .....	5
2 LITERATURE REVIEW .....	7
2.1 Fischer-Tropsch reaction mechanism .....	7
2.2 Kinetics .....	12
2.3 Cobalt catalysis .....	16
2.4 Characteristics of the Co/Al <sub>2</sub> O <sub>3</sub> system .....	17
2.4.1 Cobalt spinels .....	18
2.4.2 Effect of cobalt loading .....	19
2.4.3 Effect of calcination temperature .....	22
2.4.4 Effect of cobalt precursor .....	23
2.4.5 Promotion with noble metals .....	24
2.5 Activity and selectivity .....	30
2.5.1 Reduction extent and dispersion .....	30
2.5.2 CO hydrogenation activity .....	32
2.5.3 CO hydrogenation selectivity .....	34
2.5.4 Activity and selectivity of bimetallic systems, compared to monometallic systems .....	37
3 EXPERIMENTAL .....	43
3.1 Catalysts preparation .....	43
3.2 Temperature programmed reduction .....	46

3.2.1 Principles .....	46
3.2.2 Apparatus and procedure .....	47
3.3 Pulse O <sub>2</sub> titration .....	49
3.3.1 Principles .....	49
3.3.2 Apparatus and procedure .....	49
3.4 Volumetric chemisorption of H <sub>2</sub> and CO .....	50
3.4.1 Principles .....	50
3.4.2 Apparatus and procedure .....	51
3.5 Kinetic investigations .....	53
3.5.1 Apparatus and analytical equipment .....	53
3.5.2 Procedure for kinetic experiments .....	55
 4 RESULTS AND DISCUSSION .....	 57
4.1 Characterization of catalysts .....	57
4.1.1 Temperature programmed reduction .....	57
4.1.1.1 Influence of calcination temperature .....	57
4.1.1.2 Co <sub>3</sub> O <sub>4</sub> .....	64
4.1.1.3 Platinum promotion .....	67
4.1.1.4 Promotion with other noble metals .....	70
4.1.1.5 Reduction at standard conditions .....	76
4.1.1.6 Effect of chloride containing metal precursors .....	77
4.1.1.7 Summary of the TPR results .....	81
4.1.2 Extent of reduction determined by pulse O <sub>2</sub> -titration .....	84
4.1.3 Volumetric chemisorption of H <sub>2</sub> and CO .....	88
4.1.3.1 Effect of calcination temperature .....	88
4.1.3.2 Effect of platinum and rhenium promotion .....	90
4.1.3.3 Effect of chloride .....	99
4.1.3.4 Dispersion and crystallite size .....	102
4.1.3.5 Summary of the H <sub>2</sub> and CO adsorption measurements .....	109
4.2 Activity measurements .....	110
4.2.1 High temperature / 7 bara total pressure .....	110
4.2.2 Low temperature / 1 bara total pressure .....	122
4.2.3 Summary of the activity measurements .....	130
4.3 Selectivity measurements .....	131
4.3.1 High temperature / 7 bara total pressure .....	131
4.3.2 Low temperature / 1 bara total pressure .....	141
 5 CONCLUSIONS .....	 145

5.1 Reduction behavior .....	145
5.2 H <sub>2</sub> and CO chemisorption .....	146
5.3 Activity and selectivity .....	147
6 REFERENCES .....	149
APPENDIXES .....	157
1 Metal loading in catalysts investigated .....	159
2 Gases used in different apparatus .....	163
3 Example of an adsorption isotherm and the calculation of dispersion from chemisorption of H <sub>2</sub> on Co/Al <sub>2</sub> O <sub>3</sub> B .....	165
4 Volumetric chemisorption of H <sub>2</sub> and CO, and dispersion calculated thereof .....	169
5 BET surface and pore size distribution .....	173
6 Formulas for calculation of activity and selectivity .....	181
7 Product selectivity over the catalysts investigated .....	185





## ACKNOWLEDGEMENTS

First I wish to thank Professor Anders Holmen for his supervision, encouragement, support and patience during the course of this work.

I would also like to thank my colleagues in the Petrochemistry group at SINTEF and at the Department of Industrial Chemistry at NTH for support and good friendship. A special thank to Geir Remo Fredriksen for long discussions about banalities as well as fundamental questions, and for sharing of frustrations when they turned up. Dr. Dag Schanke and Associate Professor Edd Anders Blekkan are acknowledged for support during the course of the work, for constructive comments on the manuscript and correction of the worst linguistic errors.

---

A special thank to Associate Professor Olav Tronstad for performing the BET measurements, and to Tharald Tharaldsen for performing the XRD measurements. Ellen Ådnanes and Terje Johansen are also acknowledged for experimental assistance.

This work was made possible through the financial support from the Royal Norwegian Council for Scientific and Industrial Research through the SPUNG program, and from SINTEF Applied Chemistry.

## LIST OF SYMBOLS AND ABBREVIATIONS

A	Preexponential factor related to numbers of surface collisions
ASF	Anderson-Schulz-Flory kinetic
AES	Auger Electron Spectroscopy
B	XRD experimental line width
BET	Adsorption isotherm named after Brunauer, Emmet and Teller
DRS	Diffuse Reflectance Spectroscopy
D	Dispersion
D <sub>r</sub>	Dispersion, taking into account reduction extent
d	Particle size, diameter
E <sub>CO</sub> , E <sub>aCO</sub>	Activation energy for CO conversion [kJ/mol]
E <sub>CH<sub>4</sub></sub> , E <sub>aCH<sub>4</sub></sub>	Activation energy for CH <sub>4</sub> formation [kJ/mol]
EPR	Electron Paramagnetic Resonance
ESR	Electron Spin Resonance
EXAFS	Extended X-ray Absorption Fine Structure
eV	Electron Volt (1 eV = 1.602 · 10 <sup>-19</sup> J)
FT	Fischer-Tropsch
f	Fraction of cobalt reduced to metal, determined from O <sub>2</sub> titration
fcc	Face centered cubic
HDS	Hydrodesulfurization
hcp	Hexagonal close packed
ISS	Ion Scattering Spectroscopy
K	Scherrer constant = 0.9
K <sub>x</sub>	Total rate constant for a elementary reaction step, where x is the main product of the reaction step
k <sub>x</sub>	Rate constant for a elementary reaction step in the direction against product x
N <sub>CO</sub>	Turnover frequency for CO conversion [mol/mol·s]
N <sub>CH<sub>4</sub></sub>	Turnover frequency for CH <sub>4</sub> formation [mol/mol·s]
N <sub>s</sub>	Number of surface atoms, measured by H <sub>2</sub> chemisorption
N <sub>tot</sub>	Total number of metal atoms
n	Number of carbon atoms in the hydrocarbon product
Pt*	Pt from a chloride containing precursor
P <sub>CO</sub>	Partial pressure of CO
P <sub>H<sub>2</sub></sub>	Partial pressure of H <sub>2</sub>
r <sub>CO</sub>	Rate for CO consumption
r <sub>HC</sub>	Rate for hydrocarbon formation
r <sub>p</sub>	Chain propagation rate
r <sub>t</sub>	Chain termination rate
SIMS	Secondary Ion Mass Spectroscopy

s	Site density [atoms/Nm <sup>2</sup> ]
TEM	Transmission Electron Microscopy
TOF	Turnover Frequency [mol/mol·s]
TPR	Temperature Programmed Reduction
W <sub>n</sub>	Weight fraction of hydrocarbon product containing n carbon atoms
XAS	X-ray Absorption Spectroscopy
XPS	X-ray Photoelectron Spectroscopy
XRD	X-ray Diffraction
α	Chain growth probability
β	Broadening of the X-ray diffraction line, β = 0.20
λ	XRD wavelength, 1.5418 Å
θ	Bragg angle, 18.433
*	Surface site active for adsorption of gas molecules
[*]	Concentration of empty surface site
[x*]	Concentration of surface sites with gas x adsorbed
[*] <sub>tot</sub>	Concentration of total numbers of surface sites

## LIST OF FIGURES AND TABLES

- Figure 2-1. Product distribution of CO hydrogenation following ASF kinetic, vs. chain growth probability. From Dry /55/.
- Figure 2-2. Reaction scheme for the surface carbide mechanism. From Dry /55/.
- Figure 2-3. A general reaction scheme which has features from both the surface carbide mechanism and the CO insertion mechanism. From Dry /55/.
- Figure 2-4. TPR patterns of reference materials. From Arnoldy /3/.
- Figure 2-5. % reduction (from XRD) of  $\text{Co}/\text{Al}_2\text{O}_3$  vs. metal loading. Reduced in  $\text{H}_2$  for 4 h at  $400^\circ\text{C}$ . From /7/.
- Figure 2-6. TPR, DRS and XRD spectra of cobalt/alumina catalysts with cobalt loading from 0.1 to 16 %. Calcination temperature 773 K. From /11/.
- Figure 2-7. Scheme of the various Co phases present on 9.1%  $\text{CoO}/\text{Al}_2\text{O}_3$  as a function of calcination temperature. From Arnoldy and Moulijn /3/.
- Figure 2-8. Formation of bimetallic CoRh particles during different treatments. From van't Blik and Prins /12/.
- Figure 2-9. Dispersion, TOF,  $E_{\text{CO}}$  and  $\ln A$  for CO hydrogenation on  $\text{Co}/\text{Al}_2\text{O}_3$  catalysts of different loading. From /33/.
- Figure 2-10. Changes in TOF (from  $\text{H}_2$  ads.) with reduction extent. Reaction at 1 atm.,  $250^\circ\text{C}$ .  $\text{H}_2/\text{CO}=3$ . From /38/.
- Figure 2-11. Effect of Ir content in silica supported Co-Ir catalysts, derived from Co-acetate.  $\text{Co}:\text{Ir}:\text{SiO}_2 = 5:\text{X}:100$  /50/.
- Figure 2-12. Log rate and activation energy vs. composition.  $\text{Co-Ir}/\text{Al}_2\text{O}_3$ . From /49/.
- Figure 2-13. Selectivities for a) olefins and hydrocarbons ( $\text{C}_{2+}$ ), and b) ethylene and propylene. From /49/.
- Figure 2-14. Product selectivity and rate of  $\text{CO}/\text{H}_2$  reaction vs. bulk concentration of Co in  $\text{PtCo}/\text{Al}_2\text{O}_3$ -catalysts. From /22/.
- Figure 3-1. Outline of the combined temperature programmed analyses and pulse apparatus.
- Figure 3-2. Outline of a volumetric chemisorption apparatus/measurement. From Bergene /57/.
- Figure 3-3. Volumetric chemisorption apparatus. From Bergene /58/.

- Figure 3-4. Drawing of the catalyst bed.
- Figure 3-5. Outline of the apparatus used for kinetic investigations.
- Figure 4-1. TPR spectra of Co/Al<sub>2</sub>O<sub>3</sub>B calcined two hours at different temperatures. The straight line on the X-axis after 1173 K indicates constant temperature.
- Figure 4-2. TPR spectra of Co1.0Pt/Al<sub>2</sub>O<sub>3</sub>B calcined two hours at 573 and 648 K.
- Figure 4-3. TPR spectrum of Al<sub>2</sub>O<sub>3</sub>B.
- Figure 4-4. TPR spectra of different Co<sub>3</sub>O<sub>4</sub> catalysts compared to an alumina supported cobalt catalyst.
- Figure 4-5. TPR-spectra of Co/Al<sub>2</sub>O<sub>3</sub>A and Co/Al<sub>2</sub>O<sub>3</sub>A promoted with 0.1 and 1.0 wt % Pt. and 0.3Pt\*/Al<sub>2</sub>O<sub>3</sub>A. Calcination temperature 673 K.
- Figure 4-6. TPR spectra of Co/Al<sub>2</sub>O<sub>3</sub>A promoted with 0.1 wt% of different metals. Calcination temperature 673 K.
- Figure 4-7. TPR-spectra of Co/Al<sub>2</sub>O<sub>3</sub>B and Co/Al<sub>2</sub>O<sub>3</sub>B promoted with 1 wt% Pt or 1 wt% Re. Calcination temperature 573 K.
- Figure 4-8. TPR of Co/Al<sub>2</sub>O<sub>3</sub>B and Co/Al<sub>2</sub>O<sub>3</sub>B promoted with 1 wt% Pt or 1 wt% Re after standard reduction at 623 K for 16 h and cooling to ambient temperature.
- Figure 4-9. TPR-spectra of Co/Al<sub>2</sub>O<sub>3</sub>A and Co1.0Pt/Al<sub>2</sub>O<sub>3</sub>A catalysts with chloride (Pt\*) and without chloride (Pt). Calcination temperature 673 K.
- Figure 4-10. Exchange reactions that occur during the impregnation of platinum on alumina. a) Formation of oxychloride of platinum. b) Chloride/hydroxyl ion exchange. From Franck /72/.
- Figure 4-11. A simplified model showing the possible metal/metal oxide phases on calcined and reduced Al<sub>2</sub>O<sub>3</sub> supported cobalt catalysts, with and without a platinum promoter.
- Figure 4-12. TPR spectra of Co1.0Pt/Al<sub>2</sub>O<sub>3</sub>B at different temperature programming. a) 10 K/min, 293 to 1173 K. b) 2 K/min from 293 to 623 K, and then at constant temperature 623 K for 16 h.
- Figure 4-13. H<sub>2</sub> uptake at 298 K on Co/Al<sub>2</sub>O<sub>3</sub> catalysts calcined at different temperatures and reduced at 623 K in flowing H<sub>2</sub> for 16 hours. Support A and B.
- Figure 4-14. H<sub>2</sub> adsorption on catalysts with various platinum loading. Chloride free platinum precursor and calcination temperature 673 K.

- Figure 4-15. CO adsorption on catalysts with various platinum loading. Chloride free platinum precursor and calcination temperature 673 K.
- Figure 4-16. H<sub>2</sub> adsorption on cobalt catalysts promoted with 1 wt% chloride free Pt and Re. Calcination temperature 673 K.
- Figure 4-17. CO adsorption on cobalt catalysts promoted with 1 wt % chloride free Pt and Re. Calcination temperature 673 K.
- Figure 4-18. The ratio between CO and H uptake on different catalysts calcined at 673 K and reduced in situ at 623 K for 16 hours.
- Figure 4-19. H<sub>2</sub> adsorption on cobalt catalysts with various platinum loading. 100 % dispersion of Pt, and a Pt:H ratio of 1:1 assumed.
- Figure 4-20. H<sub>2</sub> adsorption on catalysts with various platinum loading. Chloride containing platinum precursor and calcination temperature 673 K.
- Figure 4-21. XRD analyses. Calcination at 673 K, reduction at 623 K for 16 h and passivation in O<sub>2</sub> at 298 K. a) Co(fcc): 44.19 b) Co(hcp): 47.42, 44.48, 41.59 c) CoO: 61.69, 42.99, 36.85 d)  $\gamma$ -Al<sub>2</sub>O<sub>3</sub>: 67.03, 45.86, 39.49, 37.60.
- Figure 4-22. A typical reaction run plot for the cobalt catalysts. Catalyst: Co/Al<sub>2</sub>O<sub>3</sub>A calcined at 673 K, T = 508 K, P<sub>tot</sub> = 7 bara and H<sub>2</sub>:CO = 2.
- Figure 4-23. Arrhenius plot showing the temperature dependence of the CO hydro-genation rate over Co/Al<sub>2</sub>O<sub>3</sub>A calcined at 673K. P<sub>tot</sub> = 7 bar, H<sub>2</sub>:CO=2.
- Figure 4-24. Hydrogen partial pressure dependence of the CO hydrogenation rate over Co/Al<sub>2</sub>O<sub>3</sub>A calcined at 673 K. P<sub>CO</sub>=2.3 bar, T = 513 K, P<sub>tot</sub>=7 bar.
- Figure 4-25. CO partial pressure dependence of the CO hydrogenation rate over Co/Al<sub>2</sub>O<sub>3</sub>A calcined 673 K. P<sub>H2</sub> = 4.7 bar, T = 513 K, P<sub>tot</sub> = 7 bar.
- Figure 4-26. Arrhenius plot for Co/Al<sub>2</sub>O<sub>3</sub>A and Co0.1Pt/Al<sub>2</sub>O<sub>3</sub>, P<sub>tot</sub>=7 bar, H<sub>2</sub>:CO=2, GHSV = 56000 Nml/g cat.h.
- Figure 4-27. CO conversion rate over Co/Al<sub>2</sub>O<sub>3</sub>A and Co0.1Pt/Al<sub>2</sub>O<sub>3</sub>A, both calcined at 673 K. T = 506 K, P = 7 bara and H<sub>2</sub>/CO = 2.
- Figure 4-28. CO hydrogenation activity as function of reaction time over Co/Al<sub>2</sub>O<sub>3</sub>B, Co1.0Pt/Al<sub>2</sub>O<sub>3</sub>B and Co1.0Re/Al<sub>2</sub>O<sub>3</sub>B at T=473 K, P=1 bar, H<sub>2</sub>/CO=2.
- Figure 4-29. The ratio between the activity over Re or Pt promoted catalysts and over unpromoted catalysts, as a function of reaction rate.
- Figure 4-30. Schulz-Flory plot of the hydrocarbons produced over Co/Al<sub>2</sub>O<sub>3</sub>A at 527 K and 7 bara. H<sub>2</sub>:CO ratio = 2 and CO conversion = 4.5 %.

- Figure 4-31. Chain growth probability,  $\alpha$ , over  $\text{Co}/\text{Al}_2\text{O}_3/\text{A}$  as a function of reaction time.  $T = 507 \text{ K}$ ,  $P = 7 \text{ bara}$ ,  $\text{H}_2:\text{CO} \text{ ratio} = 2$ . The CO conversion decreases from 6 to 3.5 % during the period.
- Figure 4-32. Chain growth probability,  $\alpha$ , over  $\text{Co}/\text{Al}_2\text{O}_3/\text{A}$  as a function of temperature.  $P = 7 \text{ bara}$ ,  $\text{H}_2:\text{CO} = 2$  and CO conversion = 4.5 - 7 %.
- Figure 4-33. Product distribution over  $\text{Co}/\text{Al}_2\text{O}_3/\text{A}$  as a function of temperature.  $P = 7 \text{ bara}$ ,  $\text{H}_2:\text{CO} \text{ ratio} = 2$  and CO conversion = 4.5 - 7 %.
- Figure 4-34. Product distribution over  $\text{Co}/\text{Al}_2\text{O}_3/\text{A}$  as a function of  $\text{H}_2:\text{CO}$  ratio.  $T = 511 \pm 3 \text{ K}$ ,  $P = 7 - 9 \text{ bara}$  and CO conversion = 4.5 - 6.5 %.
- Figure 4-35. Product distribution over  $\text{Co}/\text{Al}_2\text{O}_3/\text{A}$ ,  $\text{Co}0.1\text{Pt}/\text{Al}_2\text{O}_3/\text{A}$  and  $\text{Co}1.0\text{Pt}/\text{Al}_2\text{O}_3/\text{A}$  at 506 K.  $P = 7 \text{ bara}$ ,  $\text{H}_2:\text{CO} \text{ ratio} = 2$  and CO conversion = 4.5 - 5 %.
- Figure 4-36. The  $\alpha$ -olefin/n-paraffin ratio of the hydrocarbons as a function of carbon number.  $\text{Co}/\text{Al}_2\text{O}_3/\text{A}$ ,  $T = 510 \pm 3 \text{ K}$ ,  $P = 7 \text{ bara}$  and  $\text{H}_2:\text{CO} = 2$ .
- Figure 4-37.  $\alpha$ -olefin/n-paraffin ratio of the  $\text{C}_2$  and  $\text{C}_4$  fraction as a function of temperature.  $\text{Co}/\text{Al}_2\text{O}_3/\text{A}$ ,  $P = 7 \text{ bara}$ ,  $\text{H}_2:\text{CO} = 2$  and CO conversion = 4.5 - 7%.
- Figure 4-38. The  $\alpha$ -olefin/n-paraffin ratio in the  $\text{C}_2$  and  $\text{C}_4$  fraction as a function of  $\text{H}_2:\text{CO}$  ratio.  $\text{Co}/\text{Al}_2\text{O}_3/\text{A}$ ,  $T = 510 \pm 3 \text{ K}$ ,  $P = 7 - 9 \text{ bara}$  and CO conversion = 5 - 7 %.
- Figure 4-39. The  $\alpha$ -olefin/n-paraffin ratio in the  $\text{C}_2$  and  $\text{C}_4$  fraction over catalysts with increasing platinum addition.  $T = 510 \pm 3 \text{ K}$ ,  $P = 7 \text{ bara}$ ,  $\text{H}_2:\text{CO} = 2$  and CO conversion 4.5 - 7 %.
- Figure 4-40. Hydrocarbon product selectivity over  $\text{Co}/\text{Al}_2\text{O}_3/\text{A}$  with  $\text{H}_2:\text{CO} = 2$  and 3.1 at 473 K and 1 bara. GHSV = 5000 and 7000, CO conversion = 3.4 and 5.5, respectively.
- Figure 4-41. Hydrocarbon product selectivity  $\text{Co}/\text{Al}_2\text{O}_3/\text{A}$  and  $\text{Co}1.0\text{Pt}/\text{Al}_2\text{O}_3/\text{A}$  with  $\text{H}_2:\text{CO} = 3$  at 473 K and 1 bara. GHSV = 7000, CO conversion = 5.5 and 7.7 %, respectively.

Table 2-1.	Kinetic investigations.
Table 2-2.	A summary of the Co catalyst characterization literature in Chapter 2-4.
Table 2-3.	Changes in hydrocarbon product distribution with cobalt loading, reduction time and reduction temperature. From Lee et al. /38/.
Table 3-1.	BET surface and pore size data.
Table 3-2.	Catalysts used in the investigations.
Table 4-1.	Nitrogen content in catalysts calcined at 573 and 648 K.
Table 4-2.	Effect of calcination temperature on $H_2$ consumption in reduction of $Co/Al_2O_3B$ (calculated from TPR with 0.2 g of catalyst, 300-1173 K, 10 K/min, 30 ml/min of 7% $H_2$ in Ar). Calcination time is two hours.
Table 4-3.	TPR and BET results for $Co_3O_4$ .
Table 4-4.	Influence of platinum amount on $H_2$ consumption in TPR. Calcination temperature 673 K.
Table 4-5.	$H_2$ consumption in TPR. $Co/Al_2O_3$ with 0.1 wt% of different metals. Calcination temperature 673 K.
Table 4-6.	Temperature shift in TPR peaks due to Pt and Re promotion of 10% $Co/Al_2O_3$ .
Table 4-7.	Literature TPR data showing reduction temperatures (reduction peak maxima) of supported metal oxides.
Table 4-8.	Degree of reduction (%) of catalysts found by pulse $O_2$ titration at 673 K after reduction for 14 hours at 623 K. and by TPR during a corresponding reduction.
Table 4-9.	Comparison of different ways of calculating the degree of reduction of cobalt catalysts prepared by impregnation of alumina with cobalt nitrate.
Table 4-10.	Cobalt metal dispersion from volumetric chemisorption data.
Table 4-11.	Degree of reduction (%) of catalysts found by pulse $O_2$ titration at 298 K (passivation) after reduction for 14 hours at 623 K.
Table 4-12.	Comparison of cobalt dispersion (D) and particle size (d) found when using Eq. (4-1) and (4-2).
Table 4-13.	Rate as a function of promoter added to $Co/Al_2O_3A$ calcined at 673 K. Measured after 300 minutes. $T = 513$ K, $P_{tot} = 7$ bara. $H_2/CO = 2$ , GHSV = 56000 $Ncm^3/(g \text{ cat. h})$ .



Table 4-14. Activity at 473 K and 1 bara after 300 and 1400 minutes reaction time,  $H_2:CO = 2$ , GHSV =  $5000\ h^{-1}$ , CO conversion = 4-10 %.

Table 4-15. Turnover frequency (TOF) of cobalt catalysts after 5 h reaction time. T = 473 K, P = 1 bara,  $H_2:CO = 2$ , GHSV =  $5000\ h^{-1}$ , conversion = 4 - 10 %.